PHYSICAL REVIEW D **94,** 103509 (2016)

Higgs vacuum metastability in primordial inflation, preheating, and reheating

Kazunori Kohri[1,2,*] and Hiroki Matsui[2,†]

[1]*KEK Theory Center, IPNS, KEK, Tsukuba, Ibaraki 305-0801, Japan*
[2]*The Graduate University of Advanced Studies (Sokendai),Tsukuba, Ibaraki 305-0801, Japan*
(Received 8 April 2016; published 10 November 2016)

Current measurements of the Higgs boson mass and top Yukawa coupling suggest that the effective Higgs potential develops an instability below the Planck scale. If the energy scale of inflation is as high as the grand unified theory (GUT) scale, inflationary quantum fluctuations of the Higgs field can easily destabilize the standard electroweak vacuum and produce a lot of anti–de Sitter (AdS) domains. This destabilization during inflation can be avoided if a relatively large nonminimal Higgs-gravity or inflaton-Higgs coupling is introduced. Such couplings generate a large effective mass term for the Higgs, which can raise the effective Higgs potential and suppress the vacuum fluctuation of the Higgs field. After primordial inflation, however, such effective masses drops rapidly and the nonminimal Higgs-gravity or inflaton-Higgs coupling can cause large fluctuations of the Higgs field to be generated via parametric resonance, thus producing AdS domains in the preheating stage. Furthermore, thermal fluctuations of the Higgs field cannot be neglected in the proceeding reheating epoch. We discuss the Higgs vacuum fluctuations during inflation, preheating, and reheating, and show that the Higgs metastability problem is severe unless the energy scale of the inflaton potential is much lower than the GUT scale.

DOI: 10.1103/PhysRevD.94.103509

I. INTRODUCTION

With the discovery of the Higgs boson at the LHC, the standard model has been completed, and elementary particle physics has entered a new era. The recent measurements of the Higgs boson mass, $m_h = 125.09 \pm 0.21(\mathrm{stat}) \pm 0.11(\mathrm{syst})$ GeV [1–4] and top quark mass, $m_t = 173.34 \pm 0.27(\mathrm{stat}) \pm 0.71(\mathrm{syst})$ GeV [5] suggest that the running of the quartic Higgs self-coupling λ becomes negative, and the effective Higgs potential becomes unstable at the scale $\Lambda_I = 10^{10} \sim 10^{11}$ GeV [6].

If the effective Higgs potential is unstable below the Planck scale, our electroweak vacuum is metastable and should eventually decay into the true vacuum through quantum tunneling [7–9]. The time scale for this decay, however, is longer than the age of the Universe, so it was thought that the Higgs vacuum metastability does not phenomenologically have any significant impact on the observed universe [10–13]. However, recently it has been argued that the electroweak vacuum instability during inflation or at the end of inflation might threaten the existence of the Universe [14–28]. Stochastic quantum fluctuations produced during inflation can cause the Higgs field value to grow as

$$\langle h^2 \rangle \simeq \frac{H^3 t}{4\pi^2}, \tag{1}$$

where h is the value of the Higgs and H is the Hubble expansion rate (or the Hubble scale). If the Higgs field evolves beyond the instability scale Λ_I before the end of inflation, the Higgs field classically rolls down into the true vacuum and anti–de Sitter (AdS) domains are formed, which is potentially catastrophic.

Not all AdS domains generated during inflation threaten the existence of our Universe [23–25], with the significance highly depending on the number and the evolution of the AdS domains. In Ref. [25], the authors discussed how AdS domains evolve both during inflation and after the end of inflation. The Higgs AdS domains can either shrink or expand, eating other regions of the electroweak vacuum. Although high-energy-scale inflation can lead to the generation of more expanding AdS domains during inflation, such domains never take over all of the inflationary dS space, because the inflationary expansion always overcomes the expansion of the AdS domains. However, after the inflationary epoch, although some AdS domains harmlessly shrink, others expand and devour our whole Universe. This indicates that the existence of AdS domains in our observable universe is catastrophic, and so in this paper we focus on the conditions for them not to be generated.

The generation of Higgs AdS domains during inflation can be suppressed by introducing a relatively large nonminimal Higgs-gravity or inflaton-Higgs coupling. Such couplings give rise to large inflationary effective mass terms, which raise the effective Higgs potential and weaken the Higgs vacuum fluctuations [17,21,25]. However, at the end of the inflation, such mass terms drop rapidly, and

*kohri@post.kek.jp
†matshiro@post.kek.jp

become ineffective for stabilizing the Higgs field [21]. Nonminimal Higgs-gravity or inflaton-Higgs coupling can also cause large Higgs fluctuations to be generated via parametric resonance [27,28], thus producing a lot of AdS domains in the preheating stage. Moreover, thermal Higgs fluctuations are not negligible in the reheating epoch after inflation. In this paper, we analyze the vacuum fluctuations of the Higgs field during inflation, preheating, and reheating and show that the Higgs metastability is a serious problem in the inflationary universe unless the energy scale of the inflaton potential is much lower than the grand unified theory (GUT) scale or the effective Higgs potential is stabilized below the Planck scale. In this paper, we use the reduced Planck mass, $M_{\rm pl} = 2.4 \times 10^{18}$ GeV.

II. INFLATIONARY HIGGS FLUCTUATIONS AND HIGGS ADS DOMAINS

In this section, we discuss the evolution of the massless Higgs field during inflation using the Fokker-Planck equation, and determine the probability that Higgs AdS domains are formed. In the large-field regime $h \gg v$, where $v = 246$ GeV, the effective Higgs potential can be approximated by the following renormalization group (RG)-improved tree-level expression[1]:

$$V_{\rm eff}(h) = \frac{\lambda_{\rm eff}(h)}{4} h^4, \tag{2}$$

where $\lambda_{\rm eff}(h)$ is the effective self-coupling including the RG-improved couplings, the one-loop corrections. The instability scale Λ_I can be defined as the effective self-coupling $\lambda_{\rm eff}(h)$ becomes negative at the scale. In the RG-improved effective Higgs potential, the instability scale is $\Lambda_I \simeq h_{\rm max}$ where $h_{\rm max}$ defined as $V_{\rm eff}(h)$ takes its maximal value.[2]

When the Hubble scale H is smaller than the Higgs field value at the maximum of the effective Higgs potential, $h_{\rm max}$, the Higgs field can tunnel into the true vacuum via the Coleman-de Luccia instanton [32]. If the Hubble rate is as large as the maximal Higgs field value $h_{\rm max}$, the transition is dominated by the Hawking-Moss instanton [33]. The transition probability of the Higgs field during inflation can also be obtained by statistical approaches using the Fokker-Planck equation, with the result being approximately equal to that obtained using the Hawking-Moss instanton [34].

The Fokker-Planck equation describes the evolution of the probability $P(h,t)$ that the Higgs takes the value h in one Hubble horizon-size region at cosmic time t, and takes the following form:

$$\frac{\partial P}{\partial t} = \frac{\partial^2}{\partial h^2}\left(\frac{H^3}{8\pi^2}P\right) + \frac{\partial}{\partial h}\left(\frac{V'_{\rm eff}(h)}{3H}P\right), \tag{3}$$

where the prime $'$ denotes the derivative with respect to the field, i.e. $V'_{\rm eff}(h) = \frac{dV_{\rm eff}}{dh}$. According to Ref. [25], we may ignore the gradient of the effective Higgs potential $V'_{\rm eff}(h)$,[3] with assuming that the field value is $h = 0$ at $t = 0$, which gives

$$P(h,t) = \sqrt{\frac{2\pi}{H^3 t}} \exp\left(-\frac{2\pi^2}{H^3 t}h^2\right). \tag{4}$$

During inflation, if the Higgs in some region evolves to values larger than Λ_I, then it will roll into the true vacuum and a potentially dangerous AdS region will be formed. The survival probability of the electroweak vacuum at the end of inflation is estimated to be [14,25]

$$P(h < \Lambda_I, N_{\rm tot}) \equiv \int_{-\Lambda_I}^{\Lambda_I} dh P(h, t_{\rm end}), \tag{5}$$

$$= {\rm erf}\left(\frac{\sqrt{2}\pi\Lambda_I}{H\sqrt{N_{\rm tot}}}\right), \tag{6}$$

where $t_{\rm end}$ denotes the time at the end of inflation, $N_{\rm tot}$ is the total e-folding number, defined as $N_{\rm tot} = H \cdot t_{\rm end}$, and ${\rm erf}(x)$ is the error function, which for $x \gg 1$ is approximately given by

$${\rm erf}(x) \simeq 1 - \frac{1}{\sqrt{\pi}x} e^{-x^2}. \tag{7}$$

Note that the total e-folding number can be much larger than the observable e-folding number $N_{\rm hor}$, which is the number of e-foldings before the end of inflation that the largest observable scales left the horizon, i.e. we could have $N_{\rm tot} \gg N_{\rm hor}$.[4] This implies that our observable Universe is only part of the whole Universe.

$P(h,t)$ in the Fokker-Planck equation describes the probability distribution of the Higgs in one horizon-sized region [35,36]. Inflation produces many such regions, and our observable Universe contains $e^{3N_{\rm hor}}$ of them. As such, the survival probability can be estimated as

$$\{P(h < \Lambda_I, N_{\rm tot})\}^{e^{3N_{\rm hor}}} > \frac{1}{2}, \tag{8}$$

[1]The effective Higgs potential is not gauge invariant, but physical quantities extracted from the effective potential (Higgs boson mass, S-matrix elements, tunneling rates) are gauge invariant [29–31]. However, here we ignore the gauge dependence of the effective Higgs potential for simplicity.

[2]If the effective Higgs potential has large effective mass terms $m_{\rm eff}^2 h^2/2$ or includes one-loop thermal correction $\Delta V_{\rm eff}(h,T)$ at the high temperature, the instability scale does not coincide with $h_{\rm max}$, i.e. $h_{\rm max} \gtrsim \Lambda_I$, and we cannot assume $h_{\rm max} = \Lambda_I$.

[3]This assumption is reasonable for $H^2 \gtrsim 0.01 V''_{\rm eff}$.

[4]The e-folding number that corresponds to when the current horizon scale left the horizon is almost the same as that associated with large-scale cosmic background radiation (CMB) observations, and we have $N_{\rm hor} \simeq N_{\rm CMB} \simeq 60$.

which, using (6) and (7), can be approximately rewritten as

$$\left\{1-\frac{H\sqrt{N_{\rm tot}}}{\pi\sqrt{2\pi}\Lambda_I}e^{-\frac{2\pi^2\Lambda_I^2}{H^2N_{\rm tot}}}\right\}^{e^{3N_{\rm hor}}}>\frac{1}{2}. \tag{9}$$

If we set $N_{\rm hor}=60$ and $N_{\rm tot}=10^3$ in (9), we obtain the following upper bound on the Hubble scale:

$$\frac{H}{\Lambda_I}<1.1\times10^{-2}. \tag{10}$$

Alternatively, we can restrict H by using the probability that the field rolls down into the true vacuum at the end of inflation, $P(h>\Lambda_I,N_{\rm tot})$, which is given as

$$P(h>\Lambda_I,N_{\rm tot})=1-P(h<\Lambda_I,N_{\rm tot}), \tag{11}$$

$$\simeq\frac{H\sqrt{N_{\rm tot}}}{\pi\sqrt{2\pi}\Lambda_I}e^{-\frac{2\pi^2\Lambda_I^2}{H^2N_{\rm tot}}}. \tag{12}$$

Multiplying this by $e^{3N_{\rm hor}}$ gives the number of AdS domains in the local region corresponding to our observable Universe. As such, the condition that there be no AdS regions within the current horizon is expressed as

$$e^{3N_{\rm hor}}P(h>\Lambda_I,N_{\rm tot})<1, \tag{13}$$

which can be approximated as

$$e^{3N_{\rm hor}}P(h>\Lambda_I,N_{\rm tot})=\frac{H\sqrt{N_{\rm tot}}}{\pi\sqrt{2\pi}\Lambda_I}e^{3N_{\rm hor}-\frac{2\pi^2\Lambda_I^2}{H^2N_{\rm tot}}}. \tag{14}$$

Therefore, we have the upper bound on the Hubble scale,

$$\frac{H}{\Lambda_I}<\sqrt{\frac{2\pi^2}{3N_{\rm hor}N_{\rm tot}}}. \tag{15}$$

If we take $N_{\rm hor}=60$ and $N_{\rm tot}=10^3$ in (14), the upper bound on the Hubble scale is numerically found to be

$$\frac{H}{\Lambda_I}<1.1\times10^{-2}. \tag{16}$$

In Fig. 1, we plot the upper bound on H/Λ_I as a function of the total e-folding number $N_{\rm tot}$, as determined by (13). We assume that $N_{\rm hor}=60$ and that the total e-folding number is greater than $N_{\rm hor}$, i.e. $60\le N_{\rm tot}$. It is natural to consider that the total e-folding number $N_{\rm tot}$ may be huge, due to the stochastic nature of inflation, and the inflationary Higgs vacuum fluctuations grow as time goes by. Consequently, requiring the Higgs vacuum to remain stable throughout inflation puts tight constraints on the Hubble scale during inflation.

Although the AdS domains impact on the existence of our observable Universe, the expansion of AdS domains never takes over the expansion of inflationary dS space [25], and therefore, it is impossible that one AdS domain terminates the inflation on all the space of the Universe. However, If the proportion of noninflating domains or the AdS domains dominates all the space of the Universe [24,37], the inflating space would crack, and inflation comes to an end.

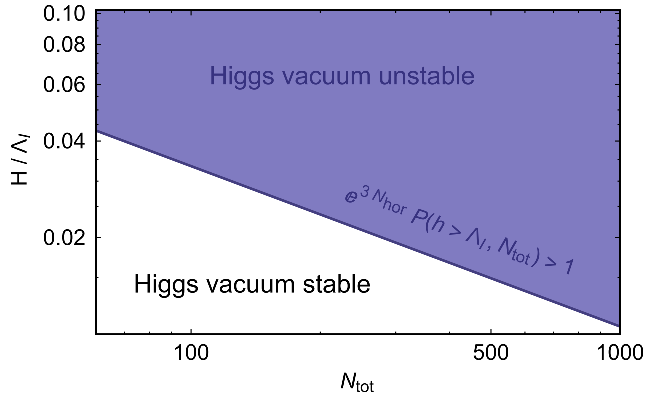

FIG. 1. Plot of the upper bound on H/Λ_I as a function of the total e-folding number $N_{\rm tot}$, as determined by (13). We set $N_{\rm hor}=60$ and $60\le N_{\rm tot}$.

III. INFLATIONARY HIGGS VACUUM FLUCTUATIONS DURING INFLATION

In the previous section we discussed the massless Higgs vacuum fluctuations during inflation, and by solving the Fokker-Planck equation we were able to determine the probability for the formation of Higgs AdS domains. In general, the inflationary Higgs fluctuations become as large as the Hubble scale H during inflation. However, if the Higgs field has a large effective mass, the Higgs vacuum fluctuations are suppressed during inflation. Field fluctuations in the massive case, particularly in the case where $m>3H/2$, have often been discussed using different descriptions in the literature. In this section we introduce mass terms for the Higgs field, determine its fluctuations, calculate the probability for the formation of Higgs AdS domains and obtain constraints on the model parameters by requiring consistency with observations.

A. Fluctuations of light Higgs field

The Friedmann-Lemaître-Robertson-Walker metric is given by

$$g_{\mu\nu}={\rm diag}\left(-1,\frac{a^2(t)}{1-Kr^2},a^2(t)r^2,a^2(t)r^2\sin^2\theta\right), \tag{17}$$

where K is the curvature constant and $a=a(t)$ is the scale factor. For simplicity we will take $K=0$. Then, the scalar curvature is obtained as

$$R=6\left[\left(\frac{\dot a}{a}\right)^2+\left(\frac{\ddot a}{a}\right)\right]. \tag{18}$$

In a de Sitter universe where $a\propto e^{Ht}$, the Ricci scalar is estimated to be $R\simeq12H^2$. We assume that the total scalar potential for the inflaton and Higgs is given as follows:

$$V(\phi, h) = V_{\rm inf}(\phi) + V_{\rm eff}(h) + \frac{1}{2}\xi h^2 R + \frac{1}{2}g^2\phi^2 h^2, \quad (19)$$

where ϕ is the inflation field, ξ is the nonminimal Higgs-gravity coupling constant, and g is the coupling constant between h and ϕ. The Klein-Gordon equation for Fourier modes of the Higgs field is given as

$$\delta\ddot{h}_k + 3H\delta\dot{h}_k + \left(\frac{k^2}{a^2} + \xi R + g^2\phi^2\right)\delta h_k = 0, \quad (20)$$

where we have assumed that we can neglect the contribution from $V_{\rm eff}(h)$ in comparison with the other terms. A finite value of ξ or g therefore generates an effective Higgs mass, which during inflation is approximately given as

$$m_{\rm eff}^2 \simeq 12H^2\xi + g^2\phi^2. \quad (21)$$

The additional Higgs mass can raise the effective Higgs potential and suppress the vacuum fluctuation of the Higgs field. The maximum of the Higgs potential gets shifted to larger values of h.

We introduce the redefined field $\delta\sigma_k$ which is related to δh_k as

$$\delta\sigma_k = a\delta h_k. \quad (22)$$

The Klein-Gordon equation for $\delta\sigma_k$ takes the form

$$\delta\sigma_k'' + \left(k^2 - \frac{1}{\tau^2}\left(\nu^2 - \frac{1}{4}\right)\right)\delta\sigma_k = 0, \quad (23)$$

where the conformal time has been introduced and is defined as $d\tau = dt/a$, and ν is defined to be

$$\nu = \sqrt{\frac{9}{4} - \frac{m_{\rm eff}^2}{H^2}}. \quad (24)$$

The general solution of Eq. (23) is expressed as

$$\delta\sigma_k = \sqrt{-\tau}[c_1 H_\nu^{(1)}(-k\tau) + c_2 H_\nu^{(2)}(-k\tau)], \quad (25)$$

where $H_{\nu\in C}^{(1)}(x)$ and $H_{\nu\in C}^{(2)}(x)$ are Hankel functions of the first and second kind.[5] In order to determine the coefficients c_1 and c_2, in the ultraviolet regime ($-k\tau \gg 1$) we match the solution with the positive-frequency plane-wave solution in flat spacetime, $e^{-ik\tau}/\sqrt{2k}$, which gives

$$c_1 = \frac{\pi}{2}e^{i(\nu+\frac{1}{2})\frac{\pi}{2}}, \qquad c_2 = 0. \quad (26)$$

The choice of a particular set of coefficients c_1, c_2 is equivalent to choosing the vacuum [38]. On superhorizon scales ($-k\tau \ll 1$), the rescaled mode functions of the Higgs take the form

$$\delta\sigma_k = \frac{\pi}{2}e^{i(\nu+\frac{1}{2})\frac{\pi}{2}}\sqrt{-\tau}H_\nu^{(1)}(-k\tau), \quad (27)$$

$$= e^{i(\nu-\frac{1}{2})\frac{\pi}{2}}2^{\nu-\frac{3}{2}}\frac{\Gamma(\nu)}{\Gamma(3/2)}\frac{1}{\sqrt{2k}}(-k\tau)^{\frac{1}{2}-\nu}. \quad (28)$$

If we consider the case where the Higgs mass is light, i.e. $m_{\rm eff} \le 3H/2$, the absolute value of δh_k is given as

$$|\delta h_k| = \frac{H}{\sqrt{2k^3}}2^{\nu-\frac{3}{2}}\frac{\Gamma(\nu)}{\Gamma(3/2)}\frac{k}{aH}\left(\frac{k}{aH}\right)^{\frac{1}{2}-\nu},$$
$$\simeq \frac{H}{\sqrt{2k^3}}\left(\frac{k}{aH}\right)^{\frac{3}{2}-\nu}. \quad (29)$$

Integrating over superhorizon modes we obtain the variance of the Higgs field fluctuations a

$$\langle h^2\rangle = \int_H^{aH}|\delta h_k|^2\frac{d^3k}{(2\pi)^3}, \quad (30)$$

$$\simeq \frac{3H^4}{8\pi^2 m_{\rm eff}^2}(m_{\rm eff} \ll 3H/2). \quad (31)$$

Next we assume that the Higgs probability distribution function is Gaussian, i.e.

$$P(h,t) = \frac{1}{\sqrt{2\pi\langle h^2\rangle}}\exp\left(-\frac{h^2}{2\langle h^2\rangle}\right). \quad (32)$$

By using Eq. (5), the probability that the standard electroweak vacuum survives can be obtained as

$$P(h < h_{\rm max}, N_{\rm tot}) \equiv \int_{-h_{\rm max}}^{h_{\rm max}} dh P(h, t_{\rm end}), \quad (33)$$

$$= {\rm erf}\left(\frac{h_{\rm max}}{\sqrt{2\langle h^2\rangle}}\right). \quad (34)$$

On the other hand, the probability that the Higgs falls into the true vacuum is expressed as

[5]The Hankel functions of the first kind asymptotically behave as

$$H_{\nu\in C}^{(1)}(x \gg 1) \sim \sqrt{\frac{2}{\pi x}}e^{i(x-\frac{\pi}{2}\nu-\frac{\pi}{4})},$$
$$H_{\nu\in R}^{(1)}(x \ll 1) \sim \left(-\frac{i}{\pi}\right)\Gamma(\nu)\left(\frac{1}{2}x\right)^{-\nu},$$
$$H_{\nu\in C}^{(1)}(x \ll 1) \sim \frac{i}{\pi\nu}\left[e^{-i\pi\nu}\Gamma(1-\nu)\left(\frac{1}{2}x\right)^{\nu} - \Gamma(1+\nu)\left(\frac{1}{2}x\right)^{-\nu}\right].$$

$$P(h > h_{\max}, N_{\rm tot}) = 1 - {\rm erf}\left(\frac{h_{\max}}{\sqrt{2\langle h^2\rangle}}\right), \tag{35}$$

$$\simeq \sqrt{\frac{2}{\pi}}\frac{\sqrt{\langle h^2\rangle}}{h_{\max}} e^{-\frac{h_{\max}^2}{2\langle h^2\rangle}}. \tag{36}$$

Imposing the condition shown in (13), we obtain the relation

$$\frac{\langle h^2\rangle}{h_{\max}^2} < \frac{1}{6N_{\rm hor}}. \tag{37}$$

If we substitute $\langle h^2\rangle$ from Eq. (31) into this relation, we find the upper bound on H to be

$$\frac{H}{h_{\max}} < \frac{2\pi m_{\rm eff}}{3H\sqrt{N_{\rm hor}}}, \tag{38}$$

which is the same as the constraint given in Ref. [25]. We plot this line in Fig. 2, where we assume $h_{\max} \sim \Lambda_I$ because of the small nonminimal coupling ξ and it is labeled by “Inflation Stage.”

B. Fluctuations of massive Higgs field

In this subsection, we consider the case of a large effective Higgs mass, namely $m_{\rm eff} > 3H/2$. We define $\tilde{\nu}$ as

$$\tilde{\nu} = \sqrt{\frac{m_{\rm eff}^2}{H^2} - \frac{9}{4}}. \tag{39}$$

On superhorizon scales, the rescaled Higgs fluctuations are given by

$$\delta\sigma_k = \frac{\pi}{2} e^{i(i\tilde{\nu}+\frac{1}{2})\frac{\pi}{2}}\sqrt{-\tau}H_{i\tilde{\nu}}^{(1)}(-k\tau). \tag{40}$$

The absolute value of $\delta\sigma_k$ is obtained as

$$|\delta\sigma_k| \simeq \frac{1}{\sqrt{2k}}(-k\tau)^{1/2}\frac{e^{\frac{\pi}{2}\tilde{\nu}}}{\sqrt{2\pi\tilde{\nu}}}|\Gamma(1-i\tilde{\nu})|. \tag{41}$$

Using the relation $|\Gamma(1-iy)|^2 = \pi y/\sinh(\pi y)$, the fluctuations of the massive Higgs field are estimated to be

$$|\delta h_k|^2 \simeq \frac{1}{2a^3\tilde{\nu}H}. \tag{42}$$

As such, the variance of the vacuum fluctuations during inflation is given as

$$\langle h^2\rangle = \int_H^{aH}|\delta h_k|^2\frac{d^3k}{(2\pi)^3} \simeq \frac{H^2}{12\pi^2\tilde{\nu}}, \tag{43}$$

$$\approx \frac{H^3}{12\pi^2 m_{\rm eff}}. \tag{44}$$

Inflationary effective mass terms thus lift the effective Higgs potential and suppress the Higgs vacuum fluctuations. Substituting the above result into (37), in the case of a massive Higgs field the requirement that our observable Universe contains no AdS domains gives us the condition

$$\frac{H}{h_{\max}} < \sqrt{\frac{2\pi^2 m_{\rm eff}}{HN_{\rm hor}}}. \tag{45}$$

The constraint on the nonminimal coupling ξ can be estimated by those conditions shown in (38) and (45). If we assume $m_{\rm eff} = \sqrt{12\xi}H$, we obtain a lower bound on the

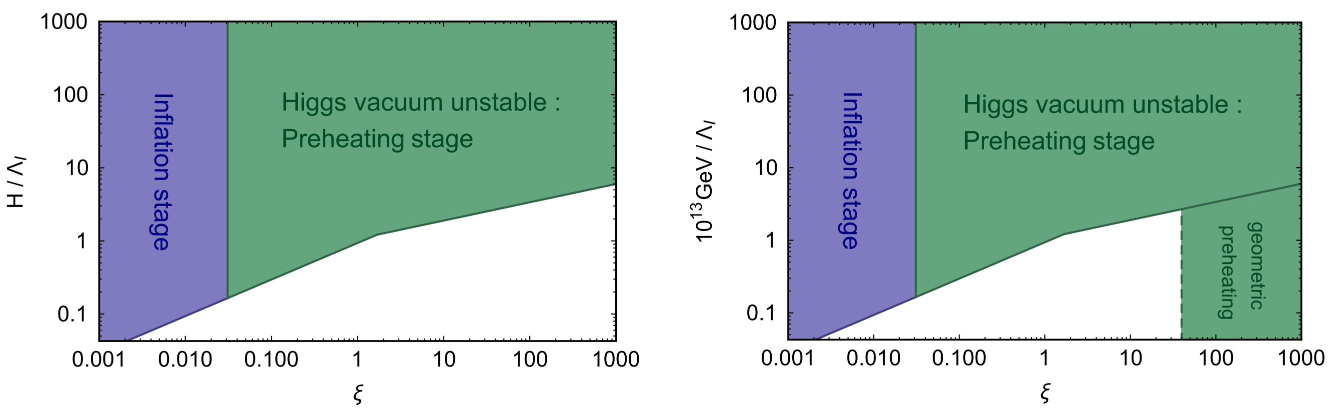

(a) nonminimal coupling ξ (b) nonminimal coupling ξ

FIG. 2. Constraints on H/Λ_I as a function of the nonminimal coupling ξ. We have plotted the lines shown in (38) and (52). We took the effective mass to be $m_{\rm eff} = \sqrt{12\xi}H$ and set $N_{\rm hor} = N_{\rm tot} = 60$. In the left panel we neglect the constraint coming from the parametric amplification of the Higgs field in order to remove model dependence. On the other hand, in the right panel we include the constraint coming from broad resonance during the preheating stage, taking the quadratic chaotic inflation model $V_{\rm inf}(\phi) \simeq \frac{1}{2}m_\phi^2\phi^2$ and the Hubble scale $H \simeq 10^{13}$ GeV as an example.

nonminimal coupling as $\xi > 0.03$ using the fact that $h_{\rm max} \simeq 10 m_{\rm eff}$.[6] This constraint corresponds to the vertical line in Fig. 2. In the case of inflaton-Higgs coupling, where $m_{\rm eff} = g\phi$, we can similarly obtain a constraint on g, but it will depend on the inflaton field value ϕ and the Hubble scale H.

While inflationary effective masses can prevent the Higgs from evolving into the true vacuum during inflation, after inflation they become ineffective, and the Higgs field fluctuations generated as a result of resonant preheating may destabilize the standard electroweak vacuum. We will discuss this problem in the next section.

IV. HIGGS FLUCTUATIONS AFTER INFLATION AND DURING THE PREHEATING STAGE

After the end of inflation, the inflaton field ϕ oscillates near the minimum of its potential and produces a huge amount of elementary particles that interact with each other and eventually form a thermal plasma. The reheating process is generally classified into several stages. In the first stage, the classical, coherently oscillating inflaton field ϕ may give rise to the production of massive bosons due to parametric resonance. In most cases, this first stage occurs extremely rapidly. This nonthermal period is called preheating [39], and is different from the subsequent stages of reheating and thermalization. Parametric resonance in the preheating stage may sometimes produce topological defects or lead to nonthermal phase transitions [40].

In Ref. [27], the authors discussed the resonant production of Higgs fluctuations after inflation in the case that the Higgs is nonminimally coupled to gravity. However, the preheating dynamics is extremely complicated, and it is difficult to estimate analytically the Higgs vacuum fluctuations during the preheating stage.[7] In this section, we numerically analyze the Higgs fluctuations after inflation and during the preheating stage. After inflation, the rescaled Higgs mode solution is no longer given by Eq. (25).[8] Instead, we use the WKB approximation and obtain the variance of the massive Higgs fluctuations which correspond with the result given by Eq. (44).

The Klein-Gordon equation for k modes of the Higgs field is given as

$$\delta\ddot{h}_k + 3H\delta\dot{h}_k + \left(\frac{k^2}{a^2} + m_{\rm eff}^2\right)\delta h_k = 0, \tag{46}$$

which can be rewritten in the useful form

$$\frac{d^2(a^{3/2}\delta h_k)}{dt^2} + \left(\frac{k^2}{a^2} + m_{\rm eff}^2 - \frac{9}{4}H^2 - \frac{3}{2}\dot{H}\right)(a^{3/2}\delta h_k) = 0. \tag{47}$$

If we consider the massive Higgs field case, i.e. $m_{\rm eff} > 3H/2$, then the Higgs mode functions are given by

$$\delta h_k \simeq \frac{e^{-i\omega_k(t)\cdot t}}{a^{3/2}\sqrt{2\omega_k(t)}}. \tag{48}$$

where $\omega_k^2 \simeq \frac{k^2}{a^2} + m_{\rm eff}^2$ and we have assumed the adiabatic condition $\dot{\omega}_k(t)/\omega_k^2(t) \ll 1$ is satisfied, and $\omega_k^2(t) > 0$. As such, the amplitude $|\delta h_k|^2$ after inflation is estimated to be [41]

$$|\delta h_k|^2 \simeq \frac{1}{2a^3\omega_k}. \tag{49}$$

Hence, the variance of the massive Higgs fluctuations which are outside the Hubble radius after inflation is given as

$$\langle h^2\rangle_{\rm end} = \frac{1}{2\pi^2}\int_0^{a_{\rm end}H_{\rm end}} k^2|\delta h_k|^2 dk, \tag{50}$$

$$\simeq \frac{H_{\rm end}^3}{12\pi^2 m_{\rm eff}}. \tag{51}$$

This can be used as an estimate for the minimum amplitude of the homogeneous Higgs field after inflation. The above Higgs fluctuations are consistent with the result

[6]The total Higgs potential during inflation can be approximated by

$$V_{\rm eff}(h) \simeq \frac{1}{2}m_{\rm eff}^2 h^2\left(1 - \frac{1}{2}\left(\frac{h}{h_{\rm max}}\right)^2\right),$$

where $h_{\rm max}$ is expressed to be

$$h_{\rm max} = \sqrt{-\frac{m_{\rm eff}^2}{\lambda_{\rm eff}}}.$$

Our assumption $h_{\rm max} \simeq 10 m_{\rm eff}$ is numerically valid for the RG-improved effective potential.

[7]The authors of Ref. [28] gave a comprehensive study of the parametric resonance of the nonminimal coupling ξ or the inflaton-Higgs coupling g by using the lattice simulations, and their results are consistent with ours.

[8]In a de Sitter background, the Klein-Gordon equation for $\delta\sigma_k$ takes the form

$$\delta\sigma_k'' + \left(k^2 - \frac{1}{\tau^2}\left(2 - \frac{m_{\rm eff}^2}{H^2}\right)\right)\delta\sigma_k = 0.$$

However, during the preheating period, if we assume that the inflaton potential is quadratic then the Universe behaves like that of a matter-dominated universe, in which case the Klein-Gordon equation takes the form

$$\delta\sigma_k'' + \left(k^2 + m_{\rm eff}^2\tau^4 - \frac{2}{\tau^2}\right)\delta\sigma_k = 0.$$

given by Eq. (44)[9] and exponentially amplified by parametric resonance. If we substitute Eq. (51) into (37), we obtain the constraint

$$\frac{H_{\rm end}}{\Lambda_I} < \sqrt{\frac{2\pi^2 m_{\rm eff}}{N_{\rm hor} H_{\rm end}}}. \tag{52}$$

Note that the effective mass [$m_{\rm eff} \simeq \sqrt{\xi R(t)}$[10] or $m_{\rm eff} \simeq g\phi(t)$] decreases and sometimes disappears during the preheating period. Therefore, the effective mass cannot stabilize the effective Higgs potential $V_{\rm eff}(h)$, and we can assume $h_{\rm max} \simeq \Lambda_I$.

Let us consider the amplification of the Higgs vacuum fluctuations via parametric resonance. For simplicity, we consider chaotic inflation with a quadratic potential as an example, i.e.

$$V_{\rm inf}(\phi) = \frac{1}{2} m_\phi^2 \phi^2, \tag{53}$$

where $m_\phi \simeq 7 \times 10^{-6} M_{\rm pl}$. In the chaotic inflation scenario, inflation occurs at super-Planckian field values, $\phi > 5M_{\rm pl}$. Primordial density perturbations relevant for the CMB are produced at around $\phi \sim 15 M_{\rm pl}$, and inflation terminates at $\phi \sim 3M_{\rm pl}$. After inflation, the inflaton field oscillates as

$$\phi(t) = \Phi(t) \sin m_\phi t, \tag{54}$$

$$\Phi(t) = \sqrt{\frac{8}{3}} \frac{M_{\rm pl}}{m_\phi t}. \tag{55}$$

When the inflaton field oscillates, the effective masses of the fluctuations of h evolve in a highly nonadiabatic way, which leads to them being produced explosively via parametric resonance.

The Klein-Gordon equation for the Higgs field given in Eq. (20) can be rewritten as

$$\frac{d^2(a^{3/2}\delta h_k)}{dt^2} + \left(\frac{k^2}{a^2} + g^2\phi^2 + \frac{1}{M_{\rm pl}^2}\left(\frac{3}{8} - \xi\right)\dot{\phi} - \frac{1}{M_{\rm pl}^2}\left(\frac{3}{4} - 4\xi\right) V(\phi)\right)(a^{3/2}\delta h_k) = 0. \tag{56}$$

Equation (56) can be reduced to the well-known Mathieu equation as follows:

$$\frac{d^2(a^{3/2}\delta h_k)}{dz^2} + (A_k - 2q\cos 2z)(a^{3/2}\delta h_k) = 0, \tag{57}$$

where $z = m_\phi t$ and A_k and q are given as

$$A_k = \frac{k^2}{a^2 m_\phi^2} + \frac{g^2\Phi^2(z)}{2m_\phi^2} + \frac{\Phi^2(z)}{2M_{\rm pl}^2}\xi, \tag{58}$$

$$q = \frac{3\Phi^2(z)}{4M_{\rm pl}^2}\left(\xi - \frac{1}{4}\right) + \frac{g^2\Phi^2(z)}{4m_\phi^2}. \tag{59}$$

The properties of the solutions to the Mathieu equation can be classified using a stability/instability chart. The solutions of the Mathieu equation show broad resonance when $q \gg 1$ or narrow resonance when $q < 1$. In the context of preheating, A_k and q are dependent on z due to the expansion of the Universe, making it very difficult to derive analytical solutions. However, we can roughly estimate δh_k by using the Floquet exponent μ_k. In the broad resonance regime, where $q \gg 1$, parametric resonance amplifies the Higgs vacuum fluctuation after inflation, giving [39,42]

$$\langle h^2 \rangle = \langle h^2 \rangle_{\rm end} \quad e^{2\pi\mu_k m_\phi t}\left(\frac{m_{\rm eff}(t_{\rm end})}{m_{\rm eff}(t)}\right)\left(\frac{H(t)}{H_{\rm end}}\right)^3, \tag{60}$$

where the Floquet exponent μ_k is given as

$$\mu_k \simeq \frac{1}{2\pi}\ln(1 + 2e^{-\pi\kappa^2}), \qquad \kappa^2 = \frac{A_k - 2q}{2\sqrt{q}}. \tag{61}$$

We can take $\kappa^2 \ll 1$ for all modes outside the horizon scale after inflation. Then we obtain $\mu_k \simeq \frac{1}{2\pi}\ln 3 \simeq 0.17$. The broad resonance requires $q \gg 1$. Therefore, the period of the broad resonance is $m_\phi t \ll \sqrt{\frac{3}{4}(\xi - \frac{1}{4}) + \frac{g^2 M_{\rm pl}^2}{4m_\phi^2}}$. Then narrow resonance follows the broad resonance.

A. Parametric resonance via nonminimal gravity-Higgs coupling ξ

In this subsection, we solve numerically the Mathieu equation in the case of geometric preheating [43,44], where $m_{\rm eff}^2$ is dominated by the ξR term. We call this the ξ-resonance scenario.[11] In this case A_k and q are given by

$$A_k \simeq \frac{k^2}{a^2 m^2} + \frac{\Phi^2(z)}{2M_{\rm pl}^2}\xi, \qquad q \simeq \frac{3\Phi^2(z)}{4M_{\rm pl}^2}\left(\xi - \frac{1}{4}\right). \tag{62}$$

[9]Note that if we consider the light Higgs field case, i.e. $m_{\rm eff} < 3H/2$, the Higgs vacuum fluctuations at the end of inflation are consistent with the result given by Eq. (31).

[10]The scalar curvature $R(t)$ is written as

$$R(t) = \frac{1}{M_{\rm pl}^2}[4V(\phi) - \dot{\phi}^2].$$

[11]In the ξ-resonance scenario, in order to obtain parametric resonance we require $\xi \gg 1$ or $\xi < 0$. The parametric amplification obtained for $\xi < 0$ is extremely strong compared with that obtained for $\xi \gg 1$ [43,44], but here we only consider positive ξ, as we are interested in the case where the effective mass acts so as to stabilize the Higgs during inflation.

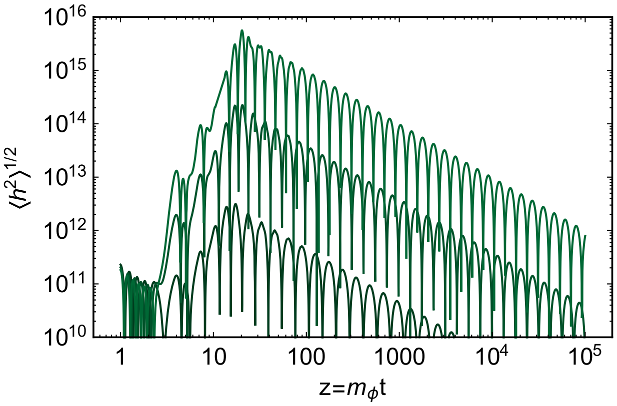

FIG. 3. Higgs vacuum fluctuation variance in the ξ-resonance scenario. In the lower, middle and upper curves we have used the nonminimal couplings $\xi = 10^{1.4}$, $\xi = 10^{1.6}$ and $\xi = 10^{1.8}$ respectively. Broad resonance occurs strongly for $\xi > 10^{1.6}$.

In Fig. 3 we show the evolution of the variance of the Higgs vacuum fluctuations as obtained by numerically solving Eq. (57) with A_k and q as given above. We take three different values for the nonminimal coupling, namely $\xi = 10^{1.4}, 10^{1.6}$ and $10^{1.8}$. We find that broad resonance can occur strongly for $\xi > 10^{1.6}$. We see that the nonminimal coupling ξ is constrained to be $\xi < 10^{1.6}$ in order not to produce the Higgs AdS domains via the parametric resonance.

B. Parametric resonance via inflaton-Higgs coupling *g*

In this subsection we solve numerically the Mathieu equation in the standard preheating scenario, where $m_{\rm eff}^2$ is dominated by the $g^2\phi^2$ term. We call this the g-resonance scenario. In this case A_k and q are given by

$$A_k \simeq \frac{k^2}{a^2 m_\phi^2} + \frac{g^2\Phi^2(z)}{2m_\phi^2}, \qquad q \simeq \frac{g^2\Phi^2(z)}{4m_\phi^2}. \tag{63}$$

In Fig. 4 we show the evolution of the variance of the Higgs vacuum fluctuations as obtained by numerically solving (57) with A_k and q given as above. For the sake of simplicity, here we have neglected backreaction effects, which we comment further on below. We consider three different values for the inflaton-Higgs coupling, namely $g = 10^{-4.4}, 10^{-4}$ and $10^{-3.6}$. Broad resonance can occur strongly for $g > 10^{-4}$. However, g is restricted in order not to give rise to large radiative corrections to the inflaton potential [45],

$$\Delta V_{\rm inf} \simeq \frac{g^4}{64\pi^2}\phi^4 \log\frac{g^2\phi^2}{m_\phi^2}. \tag{64}$$

Thus, for quadratic chaotic inflation-type models, the inflaton-Higgs coupling is constrained to be $g < 10^{-3}$. Because g resonance can occur in the parameter range $10^{-4} < g < 10^{-3}$, we find an upper bound on g as $g < 10^{-4}$.

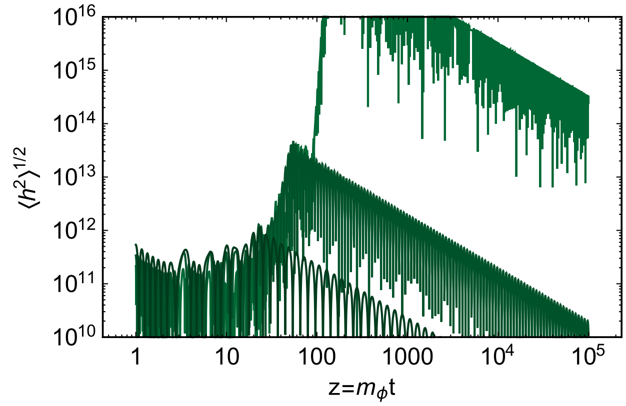

FIG. 4. Higgs vacuum fluctuation variance in the g-resonance scenario, where we ignore backreaction effects. In the lower, middle and upper curves we have used the inflaton-Higgs coupling $g = 10^{-4.4}, 10^{-4}$ and $10^{-3.6}$ respectively. Broad resonance occurs strongly for $g > 10^{-4}$.

In the early stages of parametric resonance, our semiclassical approximation is valid. On the other hand, in the later stages, backreaction effects and effects of scattering among the created particles become important (see, e.g. Ref. [46]). In this case, our semiclassical approximation may break down. However, well before the backreaction effects become significant, the generated fluctuations of the Higgs field immediately grow and exceed the hill of the effective potential due to the parametric resonance. Actually, we can estimate the maximal Higgs fluctuation $\langle h^2\rangle \sim \langle \phi^2\rangle \sim m_\phi^2/g^2$ where backreaction effects terminate the amplification of the Higgs fluctuations. The maximal Higgs fluctuation can be estimated as $\sqrt{\langle h^2\rangle} \sim m_\phi/g \sim 10^{17}$ GeV where $m_\phi \simeq 7\times 10^{-6} M_{\rm pl}$ and $g \sim 10^{-4}$ and the generated Higgs fluctuations immediately overcomes the instability scale Λ_I before the backreaction effects become significant. Therefore, the backreaction effects cannot make a significant contribution to the electroweak vacuum stability.

In Fig. 2, we plot the upper bounds on $H/h_{\rm max}$ as a function of the nonminimal gravity-Higgs coupling ξ. We have assumed that the effective mass is $m_{\rm eff} = \sqrt{12\xi}H$. In the left panel, we do not include the constraint on ξ coming from parametric amplification of the Higgs during preheating, as this constraint is model dependent, i.e. it depends on how the inflaton behaves after inflation. On the other hand, in the right panel we have included the constraint on ξ arising from broad resonance during the preheating stages. For simplicity, here we assume the quadratic chaotic inflation model with $V_{\rm inf}(\phi) = \frac{1}{2}m_\phi^2\phi^2$, which gives us the constraint $\xi < 10^{1.6}$.

V. THERMAL FLUCTUATIONS DURING THE REHEATING ERA

During the reheating stage, most of the inflaton energy is transferred to the thermal energy of elementary particles.

The reheating process finishes approximately when $H = \Gamma_{\rm tot}$. Therefore, the reheating temperature can be expressed as

$$T_{\rm reh} = \left(\frac{90}{\pi^3 g_*}\right)^{1/4} \sqrt{M_{\rm pl}\Gamma_{\rm tot}}, \tag{65}$$

where g_* is the number of relativistic degrees of freedom.[12]

Thermal effects in the reheating can raise the effective potential of the Higgs field. The RG-improved effective Higgs potential at finite temperature is given by the familiar zero-temperature corrections and the thermal corrections as

$$V_{\rm eff}(h,T) = V_{\rm eff}(h) + \Delta V_{\rm eff}(h,T). \tag{66}$$

The one-loop thermal corrections to the effective Higgs potential is given as [47–49],

$$\begin{aligned}\Delta V_{\rm eff}(h,T) &= \sum_{i=W,Z,t} \frac{n_i T^4}{2\pi^2}\int_0^\infty dk k^2 \ln\left(1 \mp e^{-\sqrt{k^2+\frac{m_i^2(h)}{T^2}}}\right), \\ &= \sum_{i=W,Z} n_i J_B(m_i,T) + \sum_{i=t} n_i J_F(m_i,T). \end{aligned} \tag{67}$$

Here we concentrate on the contributions from W bosons, Z bosons and top quarks. J_B (J_F) is the thermal bosonic (fermionic) function, $m_i(h)$ is the background-dependent mass of W, Z and t.

In Fig. 5 and Fig. 6, we plot the RG-improved effective Higgs potential at finite temperature for a range of temperatures. In Fig. 5, we plot the potential for $T = 0$ GeV and $10^{9.0}$ GeV $\le T \le 10^{10.5}$ GeV. In Fig. 6, we plot the potential for $10^{14.0}$ GeV $\le T \le 10^{15.0}$ GeV. From the figures, we see that although the high-temperature effects raise the effective potential, it cannot be stabilized up to high energy scales unless new physics emerges below the Planck scale. Therefore, if the coherent Higgs field gets over $h_{\rm max}$ during inflation or preheating stage, the generated coherent Higgs field cannot go back to the electroweak vacuum by the high-temperature effects.

In the high-temperature limit ($T \gg m_i$), the thermal bosonic (fermionic) function J_B (J_F) can be approximately written as

$$\begin{aligned} J_B(m_i,T) &\simeq -\frac{\pi^2 T^4}{90} + \frac{m_i^2 T^2}{24} - \frac{m_i^3 T}{12\pi} - \frac{m_i^4}{64\pi^2}\log\frac{m_i^2}{a_B T^2}, \\ J_F(m_i,T) &\simeq \frac{7}{8}\frac{\pi^2 T^4}{90} - \frac{m_i^2 T^2}{48} - \frac{m_i^4}{64\pi^2}\log\frac{m_i^2}{a_F T^2}, \end{aligned} \tag{68}$$

where $\log a_B \simeq 5.408$ and $\log a_F \simeq 2.635$. Here we omit the terms which are independent of h. As such, the

[12]When the effective mass of the inflaton field ϕ is too small to start to oscillate, the thermal bath is not produced. Then there would be a time lag for the production of the thermal bath until the beginning for the oscillation of the inflaton field ϕ [21]. In this case, we can adopt the constraints obtained in (52).

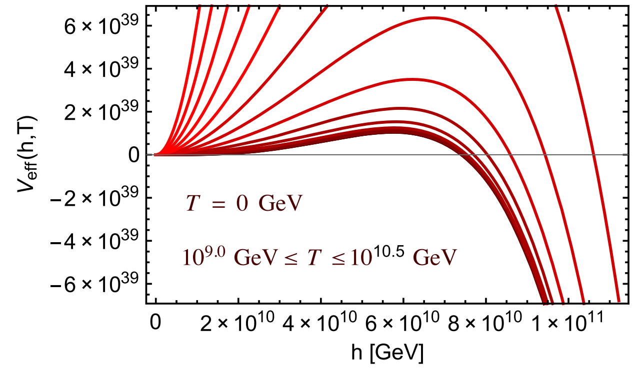

FIG. 5. RG-improved effective Higgs potential at finite temperature for $T = 0$ GeV and $10^{9.0}$ GeV $\le T \le 10^{10.5}$ GeV on the present best-fit values of m_h and m_t.

one-loop thermal corrections to the effective Higgs potential in the high-temperature limit ($T \gg m_i$) is approximately written as

$$\Delta V_{\rm eff}(h,T) \simeq \frac{1}{2}c_T T^2 h^2 + \frac{1}{3} d_T T h^3 + \frac{1}{4}\lambda_T h^4, \tag{69}$$

where

$$\begin{aligned} c_T &= \frac{3g^2 + g'^2 + 4y_t^2}{16}, \qquad d_T = \frac{6g^3 + 3(g^2+g'^2)^{3/2}}{32\pi}, \\ \lambda_T &= \frac{3}{64\pi^2}\left(-\frac{g^4}{2}\log\frac{m_W^2(h)}{a_B T^2} - \frac{(g^2+g'^2)^2}{4}\log\frac{m_Z^2(h)}{a_B T^2} \right. \\ &\quad \left. + 4y_t^4 \log\frac{m_t^2(h)}{a_F T^2}\right). \end{aligned} \tag{70}$$

The variance of the thermal fluctuations of the Higgs is given as [34,50–52]

$$\begin{aligned} \langle h^2\rangle_T &= \frac{1}{2\pi^2}\int_0^\infty \frac{k^2 dk}{\sqrt{k^2+m_{\rm eff}^2}\,[e^{\frac{\sqrt{k^2+m_{\rm eff}^2}}{T}} - 1]}, \\ &\simeq \frac{T^2}{12} - \frac{m_{\rm eff} T}{4\pi}, \end{aligned} \tag{71}$$

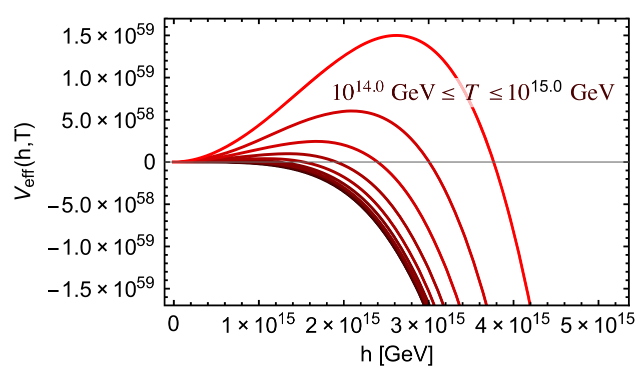

FIG. 6. RG-improved effective Higgs potential at finite temperature for $10^{14.0}$ GeV $\le T \le 10^{15.0}$ GeV. The maximum of the Higgs potential is $h_{\rm max} = 2.62T$ for $T = 10^{15.0}$ GeV.

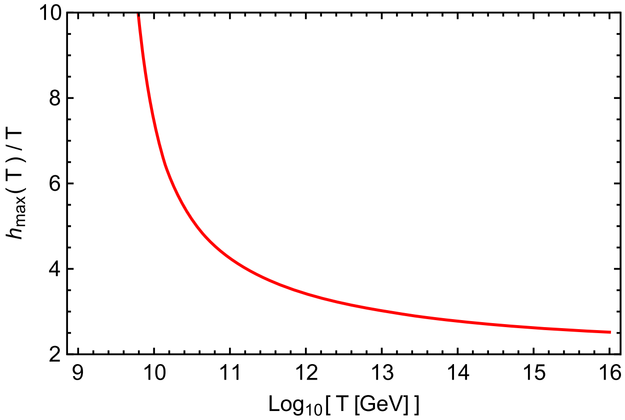

FIG. 7. Plot of $h_{\max}(T)/T$ by using RG-improved effective Higgs potential at finite temperature.

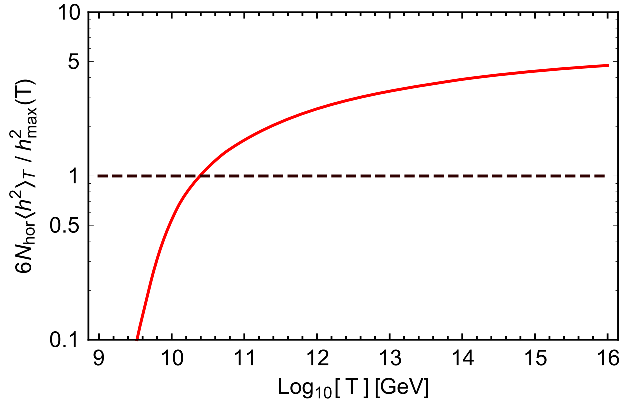

FIG. 8. We set $N_{\rm hor} = 60$ and plot $6N_{\rm hor} < h^2 >_T / h^2_{\max}(T)$ by using the RG-improved Higgs potential at the high temperature. We obtain the constraint of the temperature $T < 2.4 \times 10^{10}$ GeV.

where the thermal Higgs mass is $m_{\rm eff} = c_T^{1/2} T$ and numerically we obtain $c_T \simeq 0.2$.

We can estimate the relation with the thermal Higgs fluctuation and the physical probability of the Higgs AdS domains shown in (37) as

$$\frac{\langle h^2\rangle_T}{h^2_{\max}(T)} < \frac{1}{6N_{\rm hor}}. \tag{72}$$

The maximum of the Higgs potential is moved out to larger values of h when thermal corrections are taken into account, and numerically we have found that $h_{\max}$ can be well estimated as $h_{\max}(T) = 2 \sim 6T$. In Fig. 7, we show $h_{\max}(T)/T$ by using the RG-improved Higgs potential at the high temperature.

For simplicity, we consider the following condition:

$$\frac{6N_{\rm hor}\langle h^2\rangle_T}{h^2_{\max}(T)} < 1. \tag{73}$$

In Figs. 7 and 8, we assume $N_{\rm hor} = 60$[13] and plot $6N_{\rm hor}\langle h^2\rangle_T / h^2_{\max}(T)$ by using the RG-improved effective Higgs potential at the high temperature. When we set $N_{\rm hor} = 60$, the constraint (73) gives us the following upper bound on the temperature T:

$$T < 2.4 \times 10^{10}\ \text{GeV}. \tag{74}$$

It was previously thought that thermal Higgs fluctuations do not destabilize the standard electroweak vacuum because the probability for the thermal vacuum decay of one Hubble-sized region via the instanton methods is sufficiently small [53–56]. However, after inflation, there are the large classical Higgs field and the early universe contains huge number of independent Hubble-horizon regions. Therefore, the total decay probability due to the thermal Higgs fluctuations would be worse. Although, in this paper, we do not conclude whether the variance of the thermal Higgs fluctuation destabilizes or not, it is necessary to investigate thoroughly the thermal vacuum metastability during the reheating era. We plan to perform a detailed analysis of the stochastic approach and instanton methods in a separate paper. In the rest of this section, we assume that the variance of thermal Higgs fluctuations destabilize the standard electroweak vacuum and show how the Hubble scale H is restricted in this case.

It is known that the reheating temperature $T_{\rm reh}$ is not the maximal temperature, unless the reheating process is instantaneous. Just after inflation, although still subdominant, the decay products from the oscillating inflaton field can become thermalized and produce a so-called dilute plasma. Then, the maximal temperature $T_{\max}$ can be estimated by [57–59]

$$T_{\max} = \left(\frac{3}{8}\right)^{2/5}\left(\frac{40}{\pi^2}\right)^{1/8}\frac{g_*^{1/8}(T_{\rm reh})}{g_*^{1/4}(T_{\max})} M_{\rm pl}^{1/4} H_{\rm end}^{1/4} T_{\rm reh}^{1/2}, \tag{75}$$

with the reduced Planck mass $M_{\rm pl} = 2.4 \times 10^{18}$ GeV and $g_*(T)$ is the number of relativistic degrees of freedom at the temperature T. By using constraints (74) and assuming $T_{\rm reh} < T_{\max}$, we can obtain the upper bound on the Hubble scale H as a function of $T_{\rm reh}$.

VI. CONCLUSION

In this paper, we have discussed the stability of the Higgs vacuum during primordial inflation, preheating, and reheating. In the absence of any corrections to the Higgs potential, inflationary vacuum fluctuations of the Higgs field can easily destabilize the standard electroweak vacuum and produce a lot of AdS domains. If a relatively large nonminimal Higgs-gravity coupling or inflaton-Higgs coupling is introduced, a sizable effective mass term is

[13] $e^{3N_{\rm hor}}$ corresponds to the physical volume of our Universe at the end of the inflation.

induced, which raises the effective Higgs potential and weakens the Higgs field fluctuations. Therefore, it is possible to suppress the formation of Higgs AdS domains during inflation. However, after inflation, such effective masses are ineffective for stabilizing the large Higgs field. Moreover, nonminimal Higgs-gravity coupling and inflaton-Higgs coupling can also give rise to the generation of large Higgs fluctuations after inflaton via parametric resonance. Hence, such couplings cannot suppress the formation of Higgs AdS domains. We find that the parametric resonance during preheating excludes values of the nonminimal coupling and inflaton-Higgs coupling as $\xi < 10^{1.6}$ and $g < 10^{-4}$. Furthermore, thermal Higgs fluctuations during the reheating stage cannot be neglected on the electroweak vacuum metastability. Our results show that the thermal Higgs fluctuations produce AdS domains in the reheating stage unless $T < 2.4 \times 10^{10}$ GeV. We conclude that through the epochs of inflation, preheating and reheating, a lot of Higgs AdS domains are inevitably produced unless the energy scale of the inflaton potential is much smaller than the GUT scale, or the effective Higgs potential is stabilized below the Planck scale.

ACKNOWLEDGMENTS

We would like to thank Satoshi Iso, Kyohei Mukaida, Kazunori Nakayama, Mihoko M. Nojiri, Kengo Shimada and Jonathan White. This work is supported in part by MEXT KAKENHI Grants No. 15H05889 and No. 16H00877 (K. K.), and JSPS KAKENHI Grants No. 26105520 and No. 26247042 (K. K.). The work of K. K. is also supported by the Center for the Promotion of Integrated Science (CPIS) of Sokendai (1HB5804100).

APPENDIX: RG-IMPROVED EFFECTIVE POTENTIAL

In this appendix we provide the RG-improved effective potential for the Higgs [55,60,61], which is written in the $\overline{\text{MS}}$ scheme and in the 't Hooft-Landau gauge as

$$V_{\rm eff}(h) = V_{\rm tree}(h) + V_{1-{\rm loop}}(h). \tag{A1}$$

The improved tree-level correction to the effective Higgs potential take the form,

$$V_{\rm tree}(h) = \frac{1}{4}\lambda(t)h^4(t), \tag{A2}$$

where the running Higgs field is $h(t) = G(t)h$. The wave function renormalization factor $G(t)$ is given in terms of the anomalous dimension γ as

$$G(t) = \exp\left(-\int_0^t \gamma(t')dt'\right). \tag{A3}$$

The one-loop correction to the effective Higgs potential at zero temperature is

$$V_{1-{\rm loop}}(h) = \sum_{i=W,Z,t} \frac{n_i}{64\pi^2} m_i^4(h)\left[\ln\frac{m_i^2(h)}{\mu^2(t)} - C_i\right], \tag{A4}$$

where the number of degrees of freedom $n_i, i = W, Z, t$, and the coefficients $C_i, i = W, Z, t$ are given by

$$n_W = 6, \qquad n_Z = 3, \qquad n_t = -12,$$
$$C_W = C_Z = 5/6, \qquad C_t = 3/2. \tag{A5}$$

The masses of W, Z and t depend on the background Higgs field value h as follows:

$$m_W^2(h) = \frac{g^2(t)}{4}h^2(t), \tag{A6}$$

$$m_Z^2(h) = \frac{g^2(t) + g'^2(t)}{4}h^2(t), \tag{A7}$$

$$m_t^2(h) = \frac{y_t^2(t)}{2}h^2(t), \tag{A8}$$

where g, g' and y_t are the $SU(2)_L$, $U(1)_Y$, and top Yukawa couplings, respectively.

We calculate the β functions and the anomalous dimension γ to two-loop order in the current study. The β functions for a generic coupling parameter X are defined through the relation

$$\frac{dX(t)}{dt} = \sum_i \beta_X^{(i)}. \tag{A9}$$

The β functions and anomalous dimension γ at one- and two-loop order are given as follows [62–68]:

$$\beta_\lambda^{(1)} = \frac{1}{(4\pi)^2}\left[\lambda(-9g^2 - 3g'^2 + 12y_t^2) + 24\lambda^2 + \frac{3}{4}g^4 + \frac{3}{8}(g^2 + g'^2)^2 - 6y_t^4\right], \tag{A10}$$

$$\beta_{y_t}^{(1)} = \frac{1}{(4\pi)^2}\left[\frac{9}{2}y_t^3 + y_t\left(-\frac{9}{4}g^2 - \frac{17}{12}g'^2 - 8g_s^2\right)\right], \tag{A11}$$

$$\beta_g^{(1)} = \frac{1}{(4\pi)^2}\left[-\frac{19}{6}g^3\right], \qquad \beta_{g'}^{(1)} = \frac{1}{(4\pi)^2}\left[\frac{41}{6}g'^3\right], \beta_{g_s}^{(1)} = \frac{1}{(4\pi)^2}[-7g_s^3], \tag{A12}$$

$$\begin{aligned}\beta_\lambda^{(2)} = \frac{1}{(4\pi)^4}\bigg[&-312\lambda^3 - 144\lambda^2 y_t^2 + 36\lambda^2(3g^2+g'^2) - 3\lambda y_t^4 + \lambda y_t^2\left(\frac{45}{2}g^2 + \frac{85}{6}g'^2 + 80g_s^2\right)\\ &-\frac{73}{8}\lambda g^4 + \frac{39}{4}\lambda g^2 g'^2 + \frac{629}{24}\lambda g'^4 + 30y_t^6 - 32y_t^4 g_s^2 - \frac{9}{4}y_t^2 g^4 - \frac{8}{3}y_t^4 g'^2\\ &+\frac{21}{2}y_t^2 g^2 g'^2 - \frac{19}{4}y_t^2 g'^4 + \frac{305}{16}g^6 - \frac{289}{48}g^4 g'^2 - \frac{559}{48}g^2 g'^4 - \frac{379}{48}g'^6\bigg],\end{aligned} \tag{A13}$$

$$\begin{aligned}\beta_{y_t}^{(2)} = \frac{1}{(4\pi)^4}\bigg[y_t\bigg(&-12y_t^4 + y_t^2\left(\frac{225}{16}g^2 + \frac{131}{16}g'^2 + 36g_s^2 - 12\lambda\right) + \frac{1187}{216}g'^4\\ &-\frac{3}{4}g^2 g'^2 + \frac{19}{9}g'^2 g_s^2 - \frac{23}{4}g^4 + 9g^2 g_s^2 - 108g_s^4 + 6\lambda^2\bigg)\bigg],\end{aligned} \tag{A14}$$

$$\beta_g^{(2)} = \frac{1}{(4\pi)^4}\left[g^3\left(\frac{35}{6}g^2 + \frac{3}{2}g'^2 + 12g_s^2 - \frac{3}{2}y_t^2\right)\right], \tag{A15}$$

$$\beta_{g'}^{(2)} = \frac{1}{(4\pi)^4}\left[g'^3\left(\frac{9}{2}g^2 + \frac{199}{18}g'^2 + \frac{44}{3}g_s^2 - \frac{17}{6}y_t^2\right)\right], \tag{A16}$$

$$\beta_{g_s}^{(2)} = \frac{1}{(4\pi)^4}\left[{g_s}^3\left(\frac{9}{2}g^2 + \frac{11}{6}g'^2 - 26g_s^2 - 2y_t^2\right)\right], \tag{A17}$$

$$\gamma^{(1)} = \frac{1}{(4\pi)^2}\left[3y_t^2 - \frac{9g^2}{4} - \frac{3g'^2}{4}\right], \tag{A18}$$

$$\gamma^{(2)} = \frac{1}{(4\pi)^4}\left[6\lambda^2 - \frac{27}{4}y_t^4 + \frac{5}{2}\left(\frac{9}{4}g^2 + \frac{17}{12}g'^2 + 8g_s^2\right)y_t^2 - \frac{271}{32}g^4 + \frac{9}{16}g^2 g'^2 + \frac{431}{96}g'^4\right]. \tag{A19}$$

[1] G. Aad *et al.* (ATLAS Collaboration, CMS Collaboration), Phys. Rev. Lett. **114**, 191803 (2015).

[2] G. Aad *et al.* (ATLAS Collaboration), Phys. Lett. B **726**, 88 (2013).

[3] S. Chatrchyan *et al.* (CMS Collaboration), Phys. Rev. D **89**, 092007 (2014).

[4] P. P. Giardino, K. Kannike, I. Masina, M. Raidal, and A. Strumia, J. High Energy Phys. 05 (2014) 046.

[5] ATLAS, CDF, CMS, and D0 Collaborations, arXiv: 1403.4427.

[6] D. Buttazzo, G. Degrassi, P. P. Giardino, G. F. Giudice, F. Sala, A. Salvio, and A. Strumia, J. High Energy Phys. 12 (2013) 089.

[7] I. Yu. Kobzarev, L. B. Okun, and M. B. Voloshin, Yad. Fiz. **20**, 1229 (1974) [Sov. J. Nucl. Phys. **20**, 644 (1975)].

[8] S. R. Coleman, Phys. Rev. D **15**, 2929 (1977); **16**, 1248(E) (1977).

[9] C. G. Callan, Jr. and S. R. Coleman, Phys. Rev. D **16**, 1762 (1977).

[10] G. Degrassi, S. Di Vita, J. Elias-Miro, J. R. Espinosa, G. F. Giudice, G. Isidori, and A. Strumia, J. High Energy Phys. 08 (2012) 098.

[11] G. Isidori, G. Ridolfi, and A. Strumia, Nucl. Phys. **B609**, 387 (2001).

[12] J. Ellis, J. Espinosa, G. Giudice, A. Hoecker, and A. Riotto, Phys. Lett. B **679**, 369 (2009).

[13] J. Elias-Miro, J. R. Espinosa, G. F. Giudice, G. Isidori, A. Riotto, and A. Strumia, Phys. Lett. B **709**, 222 (2012).

[14] J. Espinosa, G. Giudice, and A. Riotto, J. Comsol. Astropart. Phys. 05 (**2008**) 002.

[15] M. Fairbairn and R. Hogan, Phys. Rev. Lett. **112**, 201801 (2014).

[16] A. Kobakhidze and A. Spencer-Smith, Phys. Lett. B **722**, 130 (2013).

[17] O. Lebedev and A. Westphal, Phys. Lett. B **719**, 415 (2013).

[18] K. Enqvist, T. Meriniemi, and S. Nurmi, J. Comsol. Astropart. Phys. 10 (**2013**) 057.

[19] M. Herranen, T. Markkanen, S. Nurmi, and A. Rajantie, Phys. Rev. Lett. **113**, 211102 (2014).

[20] A. Kobakhidze and A. Spencer-Smith, arXiv:1404.4709.
[21] K. Kamada, Phys. Lett. B **742**, 126 (2015).
[22] K. Enqvist, T. Meriniemi, and S. Nurmi, J. Comsol. Astropart. Phys. 07 (**2014**) 025.
[23] A. Hook, J. Kearney, B. Shakya, and K. M. Zurek, J. High Energy Phys. 01 (2015) 061.
[24] J. Kearney, H. Yoo, and K. M. Zurek, Phys. Rev. D **91**, 123537 (2015).
[25] J. R. Espinosa, G. F. Giudice, E. Morgante, A. Riotto, L. Senatore, A. Strumia, and N. Tetradis, J. High Energy Phys. 09 (2015) 174.
[26] C. Gross, O. Lebedev, and M. Zatta, Phys. Lett. B **753**, 178 (2016).
[27] M. Herranen, T. Markkanen, S. Nurmi, and A. Rajantie, Phys. Rev. Lett. **115**, 241301 (2015).
[28] Y. Ema, K. Mukaida, and K. Nakayama, arXiv:1602.00483.
[29] L. Di Luzio and L. Mihaila, J. High Energy Phys. 06 (2014) 079.
[30] A. Andreassen, W. Frost, and M. D. Schwartz, Phys. Rev. D **91**, 016009 (2015).
[31] A. Andreassen, W. Frost, and M. D. Schwartz, Phys. Rev. Lett. **113**, 241801 (2014).
[32] S. R. Coleman and F. De Luccia, Phys. Rev. D **21**, 3305 (1980).
[33] S. Hawking and I. Moss, Phys. Lett. **110B**, 35 (1982).
[34] A. D. Linde, Nucl. Phys. **B372**, 421 (1992).
[35] Y. Nambu, Prog. Theor. Phys. **81**, 1037 (1989).
[36] Y. Nambu and M. Sasaki, Phys. Lett. B **219**, 240 (1989).
[37] Y. Sekino, S. Shenker, and L. Susskind, Phys. Rev. D **81**, 123515 (2010).
[38] N. D. Birrell and P. C. W. Davies, *Quantum Fields in Curved Space*, Cambridge Monographs on Mathematical Physics (Cambridge University Press, Cambridge, 1984).
[39] L. Kofman, A. D. Linde, and A. A. Starobinsky, Phys. Rev. D **56**, 3258 (1997).
[40] L. Kofman, A. D. Linde, and A. A. Starobinsky, Phys. Rev. Lett. **76**, 1011 (1996).
[41] Y. Jin and S. Tsujikawa, Classical Quantum Gravity **23**, 353 (2006).
[42] A. R. Liddle, D. H. Lyth, K. A. Malik, and D. Wands, Phys. Rev. D **61**, 103509 (2000).
[43] B. A. Bassett and S. Liberati, Phys. Rev. D **58**, 021302 (1998); **60**, 049902(E) (1999).
[44] S. Tsujikawa, K.-i. Maeda, and T. Torii, Phys. Rev. D **60**, 063515 (1999).
[45] A. D. Linde, Lect. Notes Phys. **738**, 1 (2008).
[46] D. Boyanovsky, H. J. de Vega, R. Holman, and J. F. J. Salgado, Phys. Rev. D **54**, 7570 (1996).
[47] M. Carrington, Phys. Rev. D **45**, 2933 (1992).
[48] G. W. Anderson and L. J. Hall, Phys. Rev. D **45**, 2685 (1992).
[49] C. Delaunay, C. Grojean, and J. D. Wells, J. High Energy Phys. 04 (2008) 029.
[50] A. D. Linde, Rep. Prog. Phys. **42**, 389 (1979).
[51] M. Dine, R. G. Leigh, P. Y. Huet, A. D. Linde, and D. A. Linde, Phys. Rev. D **46**, 550 (1992).
[52] M. Dine, R. G. Leigh, P. Huet, A. D. Linde, and D. A. Linde, Phys. Lett. B **283**, 319 (1992).
[53] G. W. Anderson, Phys. Lett. B **243**, 265 (1990).
[54] P. B. Arnold and S. Vokos, Phys. Rev. D **44**, 3620 (1991).
[55] J. R. Espinosa and M. Quiros, Phys. Lett. B **353**, 257 (1995).
[56] L. Delle Rose, C. Marzo, and A. Urbano, J. High Energy Phys. 05 (2016) 050.
[57] D. J. Chung, E. W. Kolb, and A. Riotto, Phys. Rev. D **60**, 063504 (1999).
[58] G. F. Giudice, E. W. Kolb, and A. Riotto, Phys. Rev. D **64**, 023508 (2001).
[59] E. W. Kolb, A. Notari, and A. Riotto, Phys. Rev. D **68**, 123505 (2003).
[60] C. Ford, D. R. T. Jones, P. W. Stephenson, and M. B. Einhorn, Nucl. Phys. **B395**, 17 (1993).
[61] J. A. Casas, J. R. Espinosa, and M. Quiros, Phys. Lett. B **342**, 171 (1995).
[62] M. B. Einhorn and D. R. T. Jones, Phys. Rev. D **46**, 5206 (1992).
[63] M. E. Machacek and M. T. Vaughn, Nucl. Phys. **B249**, 70 (1985).
[64] M. E. Machacek and M. T. Vaughn, Nucl. Phys. **B236**, 221 (1984).
[65] M. E. Machacek and M. T. Vaughn, Nucl. Phys. **B222**, 83 (1983).
[66] C. Ford, I. Jack, and D. R. T. Jones, Nucl. Phys. **B387**, 373 (1992); **B504**, 551(E) (1997).
[67] M. P. Hertzberg, arXiv:1210.3624.
[68] M. Holthausen, K. S. Lim, and M. Lindner, J. High Energy Phys. 02 (2012) 037.